Basophils promote barrier dysfunction and resolution in the atopic skin

Christophe Pellefigues, Karmella Naidoo, Palak Mehta, Alfonso Schmidt, Ferdinand Jagot, Elsa Roussel, Alissa Cait, Bibek Yumnam, Sally Chappell, Kimberley Meijlink, et al.

Basophils promote barrier dysfunction and resolution in the atopic skin

Christophe Pellefigues PhD*[1,2], Karmella Naidoo PhD[1#], Palak Mehta MS[1#], Alfonso J. Schmidt MS[1#], Ferdinand Jagot MS[1], Elsa Roussel MS[3], Alissa Cait PhD[1], Bibek Yumnam MS[1], Sally Chappell MS[1], Kimberley Meijlink MS[1], Mali Camberis MS[1], Jean X. Jiang PhD[4], Gavin Painter PhD[5], Kara Filbey PhD[1], Özge Uluçkan PhD[3], Olivier Gasser PhD[1], Graham Le Gros PhD[1]

From:

1: Malaghan Institute of Medical Research, Victoria University, Wellington 6242, New Zealand

2: INSERM UMR1149, CNRS ERL8252, Centre de recherche sur l'inflammation, Inflamex, Université de Paris, Paris 75018, France

3: Novartis Institutes for Biomedical Research (NIBR), Novartis, Basel 4056, Switzerland

4: Department of biochemistry and structural biology, University of Texas Health Science Center, San Antonio TX78229, USA

5: The Ferrier Research Institute, Victoria University, Wellington 6242, New Zealand

#: These authors contributed equally

***Corresponding author:** Christophe Pellefigues, PhD, Centre de recherche sur l'inflammation, INSERM UMR1149, CNRS ERL8252, Université de Paris, Paris 75018, France.

Ph : 0033157277306, email : Christophe.pellefigues@inserm.fr

Funding

This research was funded by an independent research organization grant from the Health Research Council of New Zealand and by the Marjorie Barclay Trust (G.L.G.), and by the National Institutes of Health grant AG045040 and Welch Foundation grant AQ-1507 (J.X.J.).

Declaration of interests

25 The authors declare no competing interests

26

ABSTRACT

- **Background:** Type 2 cytokines IL-4 and IL-13 promote atopic dermatitis (AD) but also the resolution of inflammation. How type 2 cytokines participate in the resolution of AD is poorly known.
- **Objective:** To determine the mechanisms and cell types governing skin inflammation, barrier dysfunction, and the resolution of inflammation in a model of atopic dermatitis (AD)
- **Methods:** Mice reporting the expression of IL-4, IL-13, and MCPT8, or that could be deleted of basophils or eosinophils, or deficient in IL-4 or MHCII molecules, or in which basophils lack M-CSF, were treated with MC903 as an acute model of AD. Kinetics of the disease; keratinocyte differentiation; leukocyte accumulation, phenotype, function and cytokine production were measured by histopathology, molecular biology, or unbiased analysis of spectral flow cytometry.
- **Results:** Basophils were activated systemically and were the initial and main source of IL-4 in the skin in this model of AD. Basophil and IL-4 promoted epidermal hyperplasia and skin barrier dysfunction by acting on keratinocytes differentiation during inflammation. Basophil, IL-4 and basophil derived M-CSF inhibited the accumulation of pro-inflammatory cells in the skin while promoting the expansion and function of pro-resolution M2-like macrophages and the expression of pro-barrier genes. Basophils kept their pro-resolution properties during AD resolution.
- **Conclusion:** Basophils can display both beneficial and detrimental type 2 functions simultaneously during atopic inflammation.

Key Messages

- Basophils and IL-4 drive skin barrier dysfunction and keratinocyte differentiation
- Basophils M-CSF and IL-4 promote M2 expansion, efferocytosis, and resolution during atopic inflammation

KEYWORDS: Atopic dermatitis, basophils, M2, macrophages, efferocytosis, type 2 inflammation, resolution, IL-4, M-CSF.

Abbreviations: AD: Atopic dermatitis, ILC: innate lymphoid cell, TEWL: transepidermal water loss, TSLP: thymic stromal lymphopoietin,

Capsule Summary:

Basophil promotes barrier dysfunction and the resolution during murine atopic skin inflammation, partly by expressing interleukin 4 and M-CSF. Thus, basophil and interleukin 4 could play pathogenic and beneficial roles simultaneously in human atopic dermatitis.

INTRODUCTION

Atopic dermatitis (AD) is the most common chronic skin condition, affecting up to 20% of the population. It is characterized by intense itch episodes and epidermal barrier dysfunction, associated both epidemiologically and in mice models with the release of thymic stromal lymphopoietin (TSLP), IL-33, IL-4, IL-13, and histamine(1). TSLP and IL-33 can be secreted by the inflamed epidermis to directly induce the secretion of IL-4/13 by type 2 innate cells(2,3). The efficacy of Dupilumab (a monoclonal antibody targeting IL-4Rα) in AD underlines the critical functional role of IL-4 and/or IL-13 in this pathology(4).

Type 2 cytokines and histamine act on keratinocytes to prevent their timely differentiation in an ordered epidermis(5). Alongside TSLP, they also promote chronic itch through direct effects on sensory neurons(6). Keratinocyte differentiation and itch/scratch cycles are critical contributors to the epidermal hyperplasia and barrier dysfunction observed in AD(1,4). This leaky barrier enables the establishment of chronic inflammation and skin dysbiosis, and allows entry of allergens which promote the development of the atopic march(7).

Basophils are rare circulating granulocytes that can secrete type 2 cytokines and histamine(8). They exacerbate Th2 cell differentiation(9), and infiltrate the skin to activate innate lymphoid cell (ILC)2 expansion and IL-13 secretion, in AD-like disease through their secretion of IL-4(10,11). Basophils have been considered both pro-(10,12) and anti-inflammatory(13). Indeed, they infiltrate the dermis in diverse skin conditions(14), to induce epidermal hyperplasia(15,16), or support the resolution of inflammation(16–18).

Besides their pathogenic role in atopic diseases, type 2 cytokines are involved in tissue remodeling and resolution by inducing a M2 macrophage phenotype(19). M2-like macrophages contain heterogeneous subsets specialized in efferocytosis, resolution of

88 inflammation, repair and remodeling(20–22). The dermis contains several subsets of
89 macrophages, including CD64^{+} MHCII^{hi} monocyte-derived macrophages and CD64^{+} CD206^{hi}
90 dermal resident self-renewed macrophages(23,24). The expression of CD206 by
91 macrophages is induced by type 2 cytokines and is critical for the resolution of inflammation
92 and tissue remodeling through pro-inflammatory molecule scavenging and the phagocytosis
93 of collagen fibers, respectively(25,26).
94 We used an established model of AD initiated by the topical application of calcipotriol
95 (MC903) for 4 days on the ear(27), known to be dependent on epidermal TSLP
96 expression(28). This led to an acute AD-like inflammation peaking at days 9-10, followed by
97 a spontaneous resolution. Unbiased high dimensional spectral flow cytometry analysis
98 revealed that basophils were the main source of IL-4 in the skin during both inflammation
99 and its resolution. Basophil depletion, or genetic deletion of IL-4, were sufficient to delay
100 and reduce epidermal hyperplasia and barrier dysfunction. Basophils also induced the
101 expansion of M2 macrophages, efferocytosis, and pro-barrier genes, key indicators of the
102 resolution phase. Thus basophils play both pathogenic and pro-homeostatic roles in a
103 mouse model of AD.
104

Methods

Mice

6 to 12 weeks old, Basoph8 ("B8", which express the Cre recombinase and the eYFP under the control of MCPT8, specifically in basophils)(29,30), iDTR (expressing the simian Diphteria toxin receptor upon Cre activity) (31), dsRed.T3 ("dsRed", ubiquitous expression) were from Jackson Laboratories, C57BL/6J from Jackson Laboratories or Charles River Germany, iPhil (which express the simian DTR specifically in eosinophils) were from James J. Lee (Mayo Clinic Arizona)(32), IL-$4^{G4/G4}$ ("IL-4KO", express the GFP as a knockin, inactivating IL-4 expression)(33) and the 4C13R (Dual reporter of IL-4 and IL-13 expression)(30,34) were from Bill Paul (NIH), $CSF1^{fl/fl}$ were from Dr Jean X. Jiang (San Antonio University)(35), TSLPRKO mice(36) from Dr Warren Leonard (NIH) and MHCIIKO mice were gifted by Dr. Horst Bluethmann (Hoffman-La Roche, Basel)(37). All mice were bred, crossed, and housed in specific pathogen-free conditions at the Malaghan Institute of Medical Research Biomedical Research Unit or Novartis Institute for Biomedical Research Center. All experimental protocols were approved by the Victoria University of Wellington Animal Ethics Committee (Permit 24432) and performed according to local Institutional guidelines. Unless specified, only female mice were used as leucocytes and type 2 cytokine expression showed different kinetics in our models (data not shown). Littermates were used for all experiments comparing groups issued from parents with the same genotype.

Treatments

Mice were anaesthetized using intraperitoneal (i.p.) injection of ketamine/xylazine and 4nmoles of MC903 (Calcipotriol, Cayman Chemicals) in EtOH were applied daily topically for 4 days in 20µL while EtOH was applied on the contralateral ear (10µL per side). Diphtheria toxin (Cayman Chemical) was injected i.p. (20ng/g/day) to B8xiDTR and every two days to

iPhil mice(30,38). AM156 was delivered intragastrically from D0 as described(38). Apoptosis of dsRed mice splenocytes was induced in IMDM 10% FCS (Gibco) + 1µM dexamethasone at 10M/mL for 24h at 37°C 5% CO2 (>90%) and washed 3 times in excess PBS before being resuspended at $100x10^6$/mL. 20µL was then injected intradermally. 1mg of neutralizing anti-mouse IL-4 (Novartis) or rat IgG1 isotype were injected i.p. every other day.

Measurements, Histology and Microscopy

Ear thickness and TEWL were measured on sedated mice with a digital caliper (Capa System or Kroeplin) and the DERMALAB™ TEWL probe (Cortex Technology Denmark)(38) or Tewameter TM Nano (Courage+ Khazaka Electronics). Serum IgE was quantified using a mouse IgE ELISA kit (Mybiosource.com, MBS564074). Ear tissue was fixed in 4% PFA 24h, processed, paraffin embedded, sectioned at 4µm, and stained with Hematoxylin and eosin (H&E) to measure epidermal and dermal thickness or Masson's trichrome (Sigma) to measure the area of collagen as the percentage of the blue area from the total ear area using ImageJ (NIH). Images were on a widefield microscope Olympus brightfield (BX51) with a 20X NA 0.5 objective and Cell sens (Olympus). For immunofluorescence, whole ears were incubated 1h at 4°C in 20% sucrose, rinsed, snap frozen in OCT in liquid nitrogen, sectioned at 8µm, blocked in Superblock (ThermoFisher), and stained with rabbit anti-filaggrin (Poly19058), chicken anti-keratin 14 (Poly9060), rat anti-Ki-67 (16A8, both from Biolegend), and guinea pig anti-keratin 10 (Progen) overnight at 4°C. Sections were washed, stained with goat anti-rabbit IgG AF488 (A27034, Thermofisher), goat anti-chicken IgY AF647 (Ab150171, Abcam) and anti-guinea pig AF568 (ab175714, Abcam) for 2h at 4°C before being washed and mounted for confocal analysis(39). For the TUNEL assay, the Click-IT Plus TUNEL assay AF647 kit (Thermofisher) was used as per the manufacturer's guidelines, alongside DAPI. Images were recorded on an inverted microscope IX83 equipped with a

FV1200 Confocal head using a 20 X, N.A. 0.75 objective, and using FV10-ASW v4.2b (Olympus) and analyzed with ImageJ v1.52n (NIH) or Cellprofiler 3.1.8 (Broad Institute).

Tissue digestion

Blood was collected by cheek bleeding or intracardial puncture. Red blood, bone marrow, and spleen cells were lysed in an ammonium chloride buffer and prepared as already described(40). For skin cell preparations, ears were split into the dorsal and ventral layers, minced and for digested 30 minutes at 37°C in a shaking incubator (150rpm) in IMDM 5% FCS (Gibco) containing (2mg/mL) collagenase IV and (100µg/mL) DNAse I (from Sigma). Digestion was stopped by adding 5mM EDTA and a tissue filtered through a 70 µm nylon mesh filter (BD). For experiments in Fig. 7B, ears were digested using (0.25mg/mL) Liberase TM (Roche) for 20 minutes at 37°C and dissociated with the GentleMACS dissociator (Miltenyi).

Flow cytometry

Single cell suspensions were blocked for 15 min at 4°C in FACS buffer (1x PBS with 1% bovine serum albumin and 0.05% NaN_3, (Sigma)) containing 0.5% of 2.4G2 hybridoma supernatant. Cells were then stained in FACS buffer for 20 min at 4°C with an optimized panel of fluorophore-conjugated antibodies , unless specified. Antibodies used are presented in Table E1. A resume of gating strategies is represented in Table E2, and was described previously(41). Compensation was performed using UltraComp eBeads (Invitrogen) as single stained positive controls or dsRed or B8 splenocytes, and fluorescence minus one (FMO) controls were used to set background expression when needed. B8xC57 mice were used to set B8x4C13R positivity gates as FMO. Flow cytometry was performed on an Aurora spectral cytometer with 3 lasers (Cytek) or on a Fortessa X20 for Fig. 7B (BD). FACS sorting was carried out on a BD Influx™ (Becton Dickinson). T-SNE analyses were done

as Opt-SNE on default settings from at least 4 concatenated samples per group using FlowJo vX (Tree Star).

Molecular biology

For cell specific gene expression, 2000 or 10000 sort purified cells were collected in RNA lysis buffer and RNA was extracted using a Quick-RNA kit (Zymo Research). For whole skin gene expression, ears were snap frozen, minced, homogenised using 5mm stainless steel beads and a Tissue Lyzer II (Qiagen) and RNA was extracted using Trizol (Thermo Fisher) and the Quick RNA kit (Zymo Research). cDNA was synthetized using the High Capacity RNA- to-cDNA kit (Applied Biosystems). RT-qPCR was performed with a QuantStudio 7 (Applied Biosystems) and following the manufacturer's guidelines.using SYBR Green Master Mix and the following probes (*Gapdh*: F 5'- AATGGTGAAGGTCGGTGTGA, R 5'-GCAACAATCTCCACTTTGCCA; *Furin*: F 5'- ACACACAGATGAATGACAAC, R 5'-GCATTGTAAGCTACACCTAC; and *Dsg1a*: F 5'- AAGGCAGAAACGAGAATGGA, R 5' – CGAGATGCGGTATGTCACTG) or Taqman Master Mix (all from Thermo Fisher) as a duplex with probes described in Table E3. Transcript levels are expressed as the ratio of $2^{-\Delta CT}$ to GAPDH.

Statistics

Statistical analyses were performed using Prism 8 (GraphPad). Data from experimental replicates was pooled if this led to a decreased variance, or representative results from an individual experiment are represented. Parametric or non-parametric tests were used based on the normality of the data distribution assessed with a D'Agostino-Pearson K2 omnibus test. Individual dots and/or mean +/- SEM or median and the interquartile range or violin plots are shown, depending on the distribution. Post-test adjusted p values are always

represented when used. In all cases, n represents an individual mouse and a two-tailed p value < 0.05 was considered as threshold for significance.

RESULTS

1) MC903 induces an AD-like resolving epidermal pathology

After 4 days of daily MC903 treatment(27), ear thickness and transepidermal water loss (TEWL, a measure of epidermal dysfunction) continued to increase until day 9-10 before resolving, defining an inflammation (Day 0-9) and a resolution (Day 10-14) phase (Fig. 1A). Skin presentation included a redness, stiffness, shrinking, dry skin and progressive scaling of the ear (Fig. 1B). Although disease progression was associated with dermal and epidermal thickening (Fig. 1C), only epidermal swelling was associated with disease kinetics (Fig. 1D). The quantity of collagen in the dermis dropped during inflammation, before increasing during the resolution phase (Fig. 1E, F). A basal layer of $K10^-$ $K14^+$ cells (*stratum basale*, Fig. 1G, H) and a suprabasal layer of $K10^+$ $K14^+$ keratinocytes (*stratum spinosum*, Fig. 1G, I) expanded in the epidermis. $Ki67^+$ proliferating keratinocytes were found mostly in the *stratum basale* (Fig. 1J). The expression of profilaggrin (*Flg*), and an outer layer of FLG^+ keratinocytes (*stratum granulosum*) expanded over time, revealing a peak of acanthosis at D9(42). Hyperkeratosis was evident from D7 (Fig. 1C, E, G). These features were observed alongside intercellular edemas (mild spongiosis) and focal parakeratosis (Fig. E1A). Importantly, epidermal disease was more severe on the ear edges (Fig. E1B) Kinetics of collagen deposition were confirmed using picrosirius red staining (Fig. E1C, D). Thus 4 days of induction with MC903 induced a skin barrier dysfunction with some histopathological features of AD(1).

2) Basophils are the main source of type 2 cytokines in the skin

Unbiased neighbouring analysis of leukocyte kinetics measured by high dimensional spectral flow cytometry from D0 to D12 after treatment revealed 12 time-dependent clusters (Fig. 2A). The first cluster contained $CD206^{hi}$ dermal resident and $MHCII^{hi}$ monocyte derived $CD64^{hi}$ macrophages, and $CD11b^{+}$, $CD11b^{lo}$ (triple negative, TN) and $CD206^{+}CD301^{+}$ DCs ($CD64^{-}$ $CD11c^{+}$ $MHCII^{+}$). Mast cells (3), ILC2s (7), dendritic epidermal T cells (DETCs) and γδ T cells (5) were identified in the naïve skin (D0). Resident cells were stable overtime, with the exception of macrophages and DCs increasing steadily (Fig. 2A, Fig. E2A). The number of infiltrating neutrophils (2), $Ly6C^{+}$ monocytes and macrophages (9, $CD64^{low/high}$, respectively) peaked around D7, while eosinophils (10), $CD4^{+}$ and $CD8^{+}$ T cells (6), natural killer (NK) and NKT cells (8) and plasmacytoid DCs (11) peaked at D10. Basophils (4), $CD4^{-}CD8^{-}$ (DN) T cells (6) and B cells continued to increase during the resolution phase (Fig. 2B, Fig. E2B). Cluster 12 represented highly fluorescent CD45 negative cells that were excluded from further analyses. These results confirmed the kinetics of the inflammation and resolution phases (Fig. 1), and highlighted a disappearance of neutrophils, but not basophils, at the beginning of the resolution phase.

The expression of IL-4 and IL-13 in the skin was mainly restricted to basophils (4) and ILC2s (7), respectively (Fig. 2C). Only minor subsets of $CD4^{+}$ T cells were positive for IL-4 or IL-13 (Fig. 2D), contrary to the draining lymph nodes (LN) (27). Basophils were the initial and main source of IL-4 in the skin (Fig. E2C, Fig. 2C, E), while eosinophils did not show a significant expression of IL-4 or IL-13 (Fig. E2D). The proportion of $IL\text{-}13^{+}$ cells was lower than $IL\text{-}4^{+}$ cells after D7 (Fig. 2E). IL-4 gene expression outweighed IL-13 by ~10 to 100 fold from D9 to D12 (Fig. 2F). Thus, basophils were the main source of IL-4 in the skin during both inflammation and the resolution.

3) Cognate CD4$^+$ T cells and eosinophils are redundant for the induction of skin barrier dysfunction

Upon MC903 treatment, MHCII^{ko} mice(43) showed normal skin inflammation and barrier function (Fig. E3A), despite an ablation of CD4$^+$ T cells, and an increase of CD8$^+$ T cells and ILC2s in the skin (Fig. E3B).

Specific conditional depletion of eosinophils(32) impaired the development of skin inflammation but not barrier dysfunction (Fig. E3C). Eosinophils did not express IL-4 or IL-13 (Fig. 2B, D, E2D), or control the expression of IL-4 or IL-13 by basophils, ILC2s, CD4$^+$ T cells or CD206^{hi} macrophages (Fig. E3D, E3E). Overall, neither MHCII-dependent cognate CD4$^+$ T cells nor eosinophils played a non-redundant role in MC903-induced epidermal barrier dysfunction during inflammation.

4) Basophils are activated both systemically and locally in the skin

Epidermal barrier dysfunction is critical for AD disease(1), and appeared between D5 and D7 (Fig. 1A). From D4, peripheral blood and bone marrow (BM) basophils were more activated: they were bigger and overexpressed CD11b, FcεRIα, and IL-4. This systemic activation disappeared before D15 in the BM (Fig. E4A, B). Prostaglandin D2 (PGD2) mediates eosinophil recruitment and AD-like pathology in a chronic MC903 model(38), and can activate basophils systemically *in vivo*(40). However, in this acute model basophil activation and IL-4/13 expression were not inhibited by AM156, a PGD2 receptor antagonist, in the spleen or the bone marrow (Fig. E4C, D, E). TSLP is a major driver of MC903 induced AD found at D4 in the serum in this model(27,28). TSLP is known to activate murine basophils(2). MC903 did not induce basophils activation at D4 in TSLPR^{ko} mice (Fig. E4F).

Additionally, FACS-sorted TSLPR^{ko} basophils injected intradermally in MC903 treated ears did not induce an optimal skin leukocyte recruitment (Fig. E4G).

TSLP and Cyp24a1 are expressed via a direct response of keratinocytes to MC903, which ceases after treatment. Cyp24a1 codes for a member of the P450 cytochrome family involved in vitamin D metabolism(27,28). IL-3 is the most potent cytokine that can activate basophils in the skin(8). Interestingly, the expression of Cyp24a1, a gene known to be induced by TSLP in the MC903 model, decreased from D7, and from D9 IL-3 expression was dominant over TSLP, which was not detected anymore (Fig. E4H).

To explore skin and systemic basophil activation we sort-purified basophils from the spleen and the skin at D4 or D15 after MC903 treatment. Spleen basophils showed an increased expression of IL-4, IL-13, and IL-33R at D4 (but not at D15). At D4, skin basophils had a distinct phenotype and expressed more GATA3, IL-6 and amphiregulin, but less CCR3. A similar pattern was observed at D15 (Fig. E4I, J). Therefore, basophils seemed initially systemically activated by TSLP (D4-D7), but their activation was imprinted by local signals in the skin, which may include IL-3, during both the inflammation and resolution phases (D7-15).

5) Basophil and IL-4 control epidermal function and differentiation

Basophil conditional depletion(30) or IL-4 deletion did not reduce ear swelling but delayed and reduced the epidermal barrier dysfunction, which is critical to AD pathogenesis (Fig. 3A)(1). Basophil depletion reduced IL-4 gene expression by ~95% (Fig. 3B, C), confirming that basophils are the main source of IL-4 in this model (Fig. 2), and suggesting that basophil-derived IL-4 was important for the development of skin barrier dysfunction.

298 Skin barrier function is tightly controlled by keratinocyte proliferation, differentiation, and
299 cornification(1,5). Basophils and IL-4 induced epidermal hyperplasia (Fig. 3D), through an
300 expansion of Keratin 10^+ and Filaggrin$^+$ differentiated keratinocytes (*Stratum spinosum* and
301 *granulosum*) (Fig. 3E). Basophils also increased the number of proliferating $Ki67^+$ $K14^+$
302 keratinocytes, the area of the Keratin 14^+ *stratum basale* (Fig. 3F), and keratinocyte
303 differentiation (Fig. 3G).
304 These results suggested that basophils and IL-4, among other mediators, can promote
305 keratinocyte differentiation, epidermal hyperplasia and skin barrier dysfunction,
306 cornerstone features of AD(1). Basophil also promoted the differentiation of keratinocytes
307 expressing the pro-barrier genes *Flg* and *Dsg1a*(44,45).
308
309 6) **Basophil and IL-4 promote a pro-resolution leucocyte landscape during**
310 **inflammation**
311 At D9 after MC903 treatment, during inflammation, we analyzed skin leucocytes after
312 basophil depletion by performing unbiased neighboring analyses and observed 11 different
313 clusters (Fig. 4A)(41). Specific basophil conditional depletion tended to decrease mast cells,
314 and $CD206^{hi}$ and $MHCII^{hi}$ macrophages proportions (Fig. 4B, E), but increased pro-
315 inflammatory cells such as neutrophils, $CD4^+$ and $CD8^+$ T cells (Fig. 4C), and $Ly6C^+$
316 macrophages (Fig. 4D). $CD206^{hi}$ macrophages expressed IL-4 at day 9, and this proportion
317 decreased after basophil depletion (Fig. 4F)(21,25,46–48). Basophils were also associated
318 with a decrease in ILC2 IL-13 expression (Fig. 4G)(10).
319 Expression of the M2 associated markers Relmα and Arginase 1 increased from the
320 inflammation phase (D7) to the resolution phase (D12) in the skin. Basophil depletion and
321 IL-4 deletion dampened the expression of Relmα but not Arginase 1 (Fig. 4H). Basophil

depletion tended to decrease skin Alox5 expression, but not Alox8, 12 and 15, the main specialized pro-resolution mediators generating lipoxygenases(49). The expression of IL-3, IL-5, IL-6, and IL-33, but not other type 2 associated signals (IL-10, IL-18, TGFβ, amphiregulin, CCL17, M-CSF, galectin 3 and 9) also decreased after basophil depletion. Regulatory T cells (Tregs) did not seem important in the resolution, as FoxP3 expression decreased from D0 to D12 (Fig. E5A). Dermal macrophages seemed specifically biased by basophils to express more of the pro-resolution markers Alox15 and Relmα at D9 (Fig. E5B).

Overall basophils and IL-4 limited the accumulation of pro-inflammatory cells, induced M2-like macrophages and favored a pro-resolution landscape during skin inflammation.

7) Basophils control dermal resident macrophage efferocytosis

Efferocytosis is a critical step in the resolution. It is mainly carried out by $CD206^{hi}$ dermal resident macrophages, by IL-4 expressing macrophages, is induced by IL-4/13 and involves CD206 expression(22,24,46,48). Indeed, the majority of $dsRed^{+}$ apoptotic cells injected into D9 treated ears were taken up by $CD206^{hi}$ dermal resident macrophages (Fig. 5A). Basophil depletion decreased efferocytosis by skin macrophages. This was due specifically to a defect in the uptake of apoptotic cells by dermal resident $CD206^{hi}$ macrophages (Fig. 5B). $TUNEL^{+}$ apoptotic cells were observed in the epidermis in control mice (EtOH), but also in the dermis at Day 9 after MC903 treatment. The number of apoptotic cells in the skin eventually decreased during the resolution phase (Fig. 5C).

Thus, while apoptotic cells accumulated in the dermis during this AD-like inflammation, basophils promoted the pro-resolution efferocytosis function of dermal resident $CD206^{hi}$ macrophages.

346

347 8) **Basophils show pro-homeostatic properties during the resolution phase**

348 Eosinophils express lipoxygenases, and can play a pro-resolution role(50). As we failed to
349 deplete skin-infiltrated eosinophils during the resolution phase, we couldn't explore a role
350 of eosinophils in the resolution of MC903 induced skin inflammation(Fig. E6A, B, C).
351 Basophil depletion during the resolution phase lead to a small reduction in TEWL(30).
352 Unexpectedly, this was associated with an accumulation of neutrophils and $Ly6C^+$
353 monocytes, but not eosinophils (Fig. 6A). DETC, ILC2 and mast cell proportion, and IL-13
354 expression by DETCs but not by ILC2s decreased upon basophils depletion (Fig. 6B)(10).
355 Type 2 cytokine expression by $CD4^+$ T cells was unaffected (data not shown). Proportions of
356 macrophages and of $PDL2^+$ monocyte-derived M2 macrophages(51) were unchanged but
357 pro-inflammatory $Ly6C^+$ macrophages tended to accumulate after basophil depletion.
358 Similarly, macrophage expression of the resolution associated markers CD206 and IL-4 were
359 decreased(24,25,46,48) (Fig. 6C), as well as the expression of *Il4* and *Retnla* in the skin (Fig.
360 6D). Interestingly *Flg* expression and FLG+ keratinocyte numbers decreased without any
361 change in dermal or epidermal hyperplasia (Fig. 6E, F).Collagen deposition increased in the
362 dermis, as measured after Masson's trichrome staining (Fig. 6G) or picrosirius red staining
363 (data not shown). As dermal macrophages internalize and degrade collagen through CD206,
364 which is induced by IL-4, it is likely that basophils promoted this tissue remodeling through a
365 control of M2 expansion and function(26).
366 Collectively, basophils induced a M2-like macrophage bias, and a decrease of pro-
367 inflammatory cells during the resolution phase, associated with skin repair and remodeling.
368

369 9) **Both IL-4 and basophil derived M-CSF participate in the resolution**

370 IL-4 neutralization during the inflammatory phase did inhibit IgE secretion, as expected (Fig.
371 E7A). During the resolution phase, it did not inhibit the generation of IgE anymore (Fig. E7B),
372 nor did it lead to changes in ear swelling, TEWL (Fig. 7A) or total leucocyte infiltration.
373 However, IL-4 neutralization did inhibit the accumulation of neutrophils in the skin during
374 the resolution phase (Fig. 7B).
375 Basophil depletion during the inflammation phase revealed IL-4 independent effects such
376 as keratinocyte proliferation and the expansion of monocyte derived macrophages (Fig. E2,
377 E3). We looked for the genes expressed by basophils known to be associated with the
378 induction of M2 macrophages or the resolution of inflammation using a transcriptomic
379 database(52), and found lipoxygenases (*Alox5, Alox8, Alox12, Alox15*) and M-CSF were
380 potently expressed by peripheral basophils (Fig. E7C). At D9 after MC903 treatment,
381 basophils expressed similar or higher levels of pro-resolution genes as eosinophils or
382 macrophages. Besides *Il4*, they were specifically strong producers of *Alox8*, *Alox12*, *Areg*,
383 *Csf1*, *Il6* and *Tgfb1* (Fig. E7D). While skin basophil expression of *Il4* and *Il13* evolved time
384 dependently, *Csf1* expression stayed high from naïve conditions to D12 (Fig. E7E). As M-CSF
385 is important for both monocyte/macrophage and resident M2 macrophages, and shows
386 pro-repair and homeostatic functions(47,53,54), we generated the Basoph8.CSF1$^{fl/fl}$ mice
387 (CSF1$^{\Delta MCPT8}$)(30,35), in which basophils specifically show a 90% decrease of M-CSF
388 expression (Fig. E7F). Topical application of MC903 induced an exacerbated pathology with
389 an increased TEWL and/or ear swelling (Fig. 7C, D), and an altered skin immune cells
390 content: they showed fewer MHCII^{hi} and CD206^{hi} macrophages, CD4^{+} T cells, γδ T cells,
391 DETCs and ILC2s at D12 after MC903 treatment than their M-CSF-sufficient littermates.
392 CSF1$^{\Delta MCPT8}$ mice showed an accumulation of neutrophils in the skin (Fig. 7B).

393 CD206^{hi} dermal resident and infiltrating macrophage maintenance, M2 phenotype and
394 function rely on both IL-4 and M-CSF(24,47,54). Together, these results show that IL-4 and
395 basophil derived M-CSF control M2 homeostasis in an AD-like pathology. Basophils initiate
396 skin barrier dysfunction and control epidermal proliferation and differentiation after MC903
397 treatment, but also promote M2 macrophages expansion and function during skin
398 inflammation and its resolution.

DISCUSSION

Protective type 2 responses emerge following epithelial injury to expel parasites or noxious substances and thus type 2 cytokines promote a characteristic tissue phenotype including mucus secretion, remodeling, repair, and a return to homeostasis. Inappropriate or excessive type 2 responses can become pathogenic if they are not resolved, and lead to chronic itching or fibrosis(19). An intrinsic defect in the barrier function of the epidermis, observed in filaggrin or desmoglein deficiencies, can lead to excessive type 2 inflammation in the skin and to the development of AD(1,44,55). The type 2 cytokines IL-4 and/or IL-13 are critical for AD chronic inflammation, as shown by the clinical efficacy of Dupilumab, but how type 2 effector cells impair or promote the resolution of AD inflammation has not been studied(1,4).

The occurrence of AD is associated with industrialization, and environmental factors such as pollutants can lead to chronic skin barrier dysfunction and scratching (56). Such an innate chronic barrier dysfunction allows allergen entry and the development of specific adaptive atopic responses. Indeed, MC903 induces a TSLP-dependent AD-like dermatitis in the absence of functional adaptive immunity, but also promotes specific allergen sensitization through the skin(11,12,55). TSLP has been found to be more elevated in the lesional skin of pediatric cases compared to the adults(57). Most early mild pediatric cases enter remission in the first years of life, and do not show high IgE levels or positive skin prick tests to common allergens. Severe cases are more persistent and associated with allergen, commensals, or autoantigen sensitization(58–60). Thus TSLP could be an important initiator of allergen sensitization and T cell responses in infants, as in mice(9,27,61), but then become redundant once allergen sensitization is driving the disease. Indeed Tezepelumab (a TSLP neutralizing antibody) failed to improve moderate to severe adult AD over placebo

when associated with topical corticosteroids, with most patients showing high total IgE titers >150kU/L(62). Epithelial derived cytokines such as TSLP or IL-33 can trigger IL-4 and IL-13 expression by basophils, mast cells, eosinophils or ILC2s(63–65). These mechanisms could be more important for AD initiation during infancy than for skin inflammation in adulthood, when potent specific T cells and IgE responses are already established and dominant.

Here we characterized a common model of TSLP-dependent dermatitis . Mice developed a self-resolving AD-like disease histologically closer to acute than adult chronic AD. MC903 treatment was not associated with allergens(12,66), in order to study the mechanisms leading to barrier dysfunction prior to allergen sensitization. In this regard, this model differed from human AD, which is strongly associated with specific CD4+ T cell responses, whereas we did not observe a MHCII dependent skin phenotype, despite the central expansion of Th2/Th13 cells occurring in this model(27). CD4+ cells were also redundant to induce skin inflammation in a chronic model of MC903 induced AD. Importantly, in this chronic model, skin barrier function was determined by eosinophils and PGD2(38), which differs from the acute situation described here. Another limitation of this study is that the remission of human AD inflammation is usually controlled by weeks of corticosteroid treatment, whereas we studied a model showing a spontaneous resolution after the removal of the chemical offending the skin.

Immune cell recruitment to the inflamed skin tracked closely with keratinocyte differentiation and skin pathology kinetics. Contrary to pro-inflammatory cells, IL-4 producing basophils remained in the skin during the resolution phase. Basophils were activated systemically during the initiation of the disease, and were recruited to the dermis to promote keratinocyte proliferation and differentiation, and to accelerate a skin barrier

dysfunction in a partially IL-4 dependent manner. However, their role could not be described as pro-inflammatory or pathogenic: they also promoted the expansion and function of M2-like macrophages, and the expression of pro-barrier genes such as *Flg* and *Dsg1a*, during the inflammation phase.During the resolution phase, basophils supported a pro-resolution macrophage phenotype, a decrease in pro-inflammatory cells, epidermal repair and tissue remodeling. This late support seemed to rely on basophil IL-4 and M-CSF expression. Both pro-inflammatory and pro-resolution roles have been attributed to basophils during IgE mediated chronic and prurigo-like skin inflammation(16,18). However, in a liver infection model dominated by type 1 inflammation, basophils showed only some pro-resolution properties (17). Indeed, any basophil pro-homeostatic properties seem hidden by the deleterious effects of type 2 inflammation during atopy or allergy.

This homeostatic role of basophils has been associated with resident dermal macrophages in our current study, with monocyte derived macrophages during IgE mediated skin inflammation(16,18), with Kupffer cells during liver infection(17), and with alveolar macrophages during lung development(67). If basophils seem specialized to interact with distinct macrophages subsets, they also express numerous ligands able to interact with non-hematopoietic cells(67). Basophils can induce keratinocyte proliferation and differentiation(15), but they also control the activation of fibroblasts(68,69) and endothelial cells(70) via their secretion of IL-4 and histamine. As IL-4 has been shown to decrease keratinocyte differentiation and Flg expression in vitro, it is likely that basophils and IL-4 promoted keratinocytes differentiation and Flg expression through indirect effects in the current model in vivo, for example as a counterbalancing response to increased scratching. Further investigation is needed to understand if basophils can directly contribute to tissue remodeling and repair.

Cardinal immunological features of AD include an expansion of Th2 cells, eosinophils and ILC2s in the skin, all of which have been observed in various MC903 induced AD-like models(10,27,71). Surprisingly, eosinophils or cognate T cells did not represent a major source of IL-4/13 in the current model. Hence, our data supports the notion that basophil type 2 cytokine production can initiate an innate AD-like pathology.

Thus, basophils can promote a pleiotropic type 2 program inducing both a detrimental skin barrier dysfunction, and beneficial efferocytosis, repair and remodeling through their control of keratinocyte and dermal macrophage functional phenotypes.

Acknowledgements

The authors wish to thank the expert support of the Malaghan Institute of Medical Research Hugh Green Cytometry Centre, Research Information Technologies and Biomedical Research Unit staff. We want to sincerely thank Dr Warren Leonard, Dr Elizabeth Jacobsen, the Lee Lab and Dr Horst Bluethmann for mice strains and Dr Franca Ronchese for reagents. We are extremely grateful to Pr Graham Ogg and Dr Mei Li for critical discussions.

Authors contribution

Conceptualization, C.P. and G.L.G. ; Methodology, C.P., K.N., A.S. ; Investigation, C.P., K.N., A.S., P.M., F.J., E.R., A.C., S.C., K.M. ; Resources, B.Y., M.C., G.P., J.X.J., G.L.G.; Formal analysis, C.P., A.S., F.J., E.R.; Writing – original draft, C.P.; Writing – review and editing, C.P., K.F., O.U., O.G.; Supervision, C.P., K.F., O.U., O.G. and G.L.G.; Funding acquisition, J.X.J., O.G. and G.L.G.

References

1. Weidinger S, Beck LA, Bieber T, Kabashima K, Irvine AD. Atopic dermatitis. Nat Rev Dis Prim [Internet]. 2018 Dec 21 [cited 2019 May 2];4(1):1. Available from: http://www.nature.com/articles/s41572-018-0001-z

2. Siracusa MC, Saenz SA, Hill DA, Kim BS, Headley MB, Doering TA, et al. TSLP promotes interleukin-3-independent basophil haematopoiesis and type 2 inflammation. Nature [Internet]. 2011 Sep 14 [cited 2013 Feb 27];477(7363):229–33. Available from: https://www.doi.org/10.1038/nature10329

3. Liew FY, Girard J-P, Turnquist HR. Interleukin-33 in health and disease. Nat Rev Immunol [Internet]. 2016 Nov 19;16(11):676–89. Available from: http://www.nature.com/doifinder/10.1038/nri.2016.95

4. Harb H, Chatila TA. Mechanisms of Dupilumab. Clin Exp Allergy [Internet]. 2020 Jan 30;50(1):5–14. Available from: https://onlinelibrary.wiley.com/doi/abs/10.1111/cea.13491

5. Omori-Miyake M, Yamashita M, Tsunemi Y, Kawashima M, Yagi J. In Vitro Assessment of IL-4- or IL-13-Mediated Changes in the Structural Components of Keratinocytes in Mice and Humans. J Invest Dermatol [Internet]. 2014 May [cited 2019 Mar 25];134(5):1342–50. Available from: https://linkinghub.elsevier.com/retrieve/pii/S0022202X15367579

6. Oetjen LK, Mack MR, Feng J, Whelan TM, Niu H, Guo CJ, et al. Sensory Neurons Co-opt Classical Immune Signaling Pathways to Mediate Chronic Itch. Cell [Internet]. 2017;171(1):217-228.e13. Available from: http://linkinghub.elsevier.com/retrieve/pii/S0092867417309315

7. Hill DA, Spergel JM. The atopic march. Ann Allergy, Asthma Immunol [Internet]. 2018

518 Feb [cited 2019 Sep 19];120(2):131–7. Available from:
519 http://www.ncbi.nlm.nih.gov/pubmed/29413336
520 8. Karasuyama H, Miyake K, Yoshikawa S, Yamanishi Y. Multifaceted roles of basophils in
521 health and disease. J Allergy Clin Immunol [Internet]. 2018 Aug 1 [cited 2019 May
522 14];142(2):370–80. Available from: https://doi.org/10.1016/j.jaci.2017.10.042
523 9. Leyva-Castillo JM, Hener P, Michea P, Karasuyama H, Chan S, Soumelis V, et al. Skin
524 thymic stromal lymphopoietin initiates Th2 responses through an orchestrated
525 immune cascade. Nat Commun [Internet]. 2013 Dec 28 [cited 2018 Aug 8];4(1):2847.
526 Available from: http://www.nature.com/articles/ncomms3847
527 10. Kim BS, Wang K, Siracusa MC, Saenz SA, Brestoff JR, Monticelli LA, et al. Basophils
528 Promote Innate Lymphoid Cell Responses in Inflamed Skin. J Immunol [Internet].
529 2014;193(7):3717–25. Available from:
530 http://www.jimmunol.org/lookup/doi/10.4049/jimmunol.1401307
531 11. Hussain M, Borcard L, Walsh KP, Pena Rodriguez M, Mueller C, Kim BS, et al. Basophil-
532 derived IL-4 promotes epicutaneous antigen sensitization concomitant with the
533 development of food allergy. J Allergy Clin Immunol [Internet]. 2018;141(1):223-
534 234.e5. Available from:
535 http://linkinghub.elsevier.com/retrieve/pii/S0091674917305663
536 12. Noti M, Kim BS, Siracusa MC, Rak GD, Kubo M, Moghaddam AE, et al. Exposure to
537 food allergens through inflamed skin promotes intestinal food allergy through the
538 thymic stromal lymphopoietin-basophil axis. J Allergy Clin Immunol [Internet].
539 2014;133(5):1390-1399.e6. Available from:
540 http://dx.doi.org/10.1016/j.jaci.2014.01.021
541 13. Schwartz C, Eberle JU, Hoyler T, Diefenbach A, Lechmann M, Voehringer D. Opposing

functions of thymic stromal lymphopoietin-responsive basophils and dendritic cells in a mouse model of atopic dermatitis. J Allergy Clin Immunol [Internet]. 2016 Jun;138(5):1443-1446.e8. Available from: http://linkinghub.elsevier.com/retrieve/pii/S0091674916304225

14. Borriello F, Granata F, Marone G. Basophils and skin disorders. J Invest Dermatol [Internet]. 2014 May [cited 2014 Apr 28];134(5):1202–10. Available from: http://www.ncbi.nlm.nih.gov/pubmed/24499736

15. Hayes MD, Ward S, Crawford G, Seoane RC, Jackson WD, Kipling D, et al. Inflammation-induced IgE promotes epithelial hyperplasia and tumour growth. Elife [Internet]. 2020 Jan 14 [cited 2020 Jan 15];9. Available from: https://doi.org/10.7554/eLife.51862

16. Hashimoto T, Satoh T, Yokozeki H. Protective Role of STAT6 in Basophil-Dependent Prurigo-like Allergic Skin Inflammation. J Immunol [Internet]. 2015 May 15 [cited 2018 Jun 14];194(10):4631–40. Available from: http://www.ncbi.nlm.nih.gov/pubmed/25862819

17. Blériot C, Dupuis T, Jouvion G, Eberl G, Disson O, Lecuit M. Liver-Resident Macrophage Necroptosis Orchestrates Type 1 Microbicidal Inflammation and Type-2-Mediated Tissue Repair during Bacterial Infection. Immunity [Internet]. 2015 Dec 25 [cited 2015 Jan 13];1–14. Available from: http://linkinghub.elsevier.com/retrieve/pii/S1074761314004877

18. Egawa M, Mukai K, Yoshikawa S, Iki M, Mukaida N, Kawano Y, et al. Inflammatory monocytes recruited to allergic skin acquire an anti-inflammatory M2 phenotype via basophil-derived interleukin-4. Immunity [Internet]. 2013 Mar 21 [cited 2014 Oct 16];38(3):570–80. Available from: http://www.ncbi.nlm.nih.gov/pubmed/23434060

19. Gieseck RL, Wilson MS, Wynn TA. Type 2 immunity in tissue repair and fibrosis. Nat Rev Immunol [Internet]. 2018 Jan 1 [cited 2020 Jan 16];18(1):62–76. Available from: http://www.ncbi.nlm.nih.gov/pubmed/28853443

20. Wynn TA, Vannella KM. Macrophages in Tissue Repair, Regeneration, and Fibrosis. Immunity [Internet]. 2016;44(3):450–62. Available from: http://dx.doi.org/10.1016/j.immuni.2016.02.015

21. Proto JD, Doran AC, Gusarova G, Yurdagul A, Sozen E, Subramanian M, et al. Regulatory T Cells Promote Macrophage Efferocytosis during Inflammation Resolution. Immunity [Internet]. 2018 Oct 16 [cited 2018 Nov 14];49(4):666-677.e6. Available from: http://www.ncbi.nlm.nih.gov/pubmed/30291029

22. Bosurgi L, Cao YG, Cabeza-Cabrerizo M, Tucci A, Hughes LD, Kong Y, et al. Macrophage function in tissue repair and remodeling requires IL-4 or IL-13 with apoptotic cells. Science (80-) [Internet]. 2017 Jun 9;356(6342):1072–6. Available from: http://www.sciencemag.org/lookup/doi/10.1126/science.aai8132

23. Chakarov S, Lim HY, Tan L, Lim SY, See P, Lum J, et al. Two distinct interstitial macrophage populations coexist across tissues in specific subtissular niches. Science (80-) [Internet]. 2019 Mar 15;363(6432):eaau0964. Available from: http://www.sciencemag.org/lookup/doi/10.1126/science.aau0964

24. Lee SH, Charmoy M, Romano A, Paun A, Chaves MM, Cope FO, et al. Mannose receptor high, M2 dermal macrophages mediate nonhealing Leishmania major infection in a Th1 immune environment. J Exp Med [Internet]. 2018 Jan 2 [cited 2019 Apr 23];215(1):357–75. Available from: http://www.ncbi.nlm.nih.gov/pubmed/29247046

25. Lee SJ, Evers S, Roeder D, Parlow AF, Risteli J, Risteli L, et al. Mannose receptor-

590 mediated regulation of serum glycoprotein homeostasis. Science [Internet]. 2002 Mar
591 8 [cited 2018 Jul 20];295(5561):1898–901. Available from:
592 http://www.ncbi.nlm.nih.gov/pubmed/11884756
593 26. Madsen DH, Leonard D, Masedunskas A, Moyer A, Jürgensen HJ, Peters DE, et al. M2-
594 like macrophages are responsible for collagen degradation through a mannose
595 receptor–mediated pathway. J Cell Biol [Internet]. 2013 Sep 16 [cited 2019 Sep
596 19];202(6):951. Available from: http://www.ncbi.nlm.nih.gov/pubmed/24019537
597 27. Ochiai S, Jagot F, Kyle RL, Hyde E, White RF, Prout M, et al. Thymic stromal
598 lymphopoietin drives the development of IL-13 + Th2 cells. Proc Natl Acad Sci
599 [Internet]. 2018 Jan 30;115(5):1033–8. Available from:
600 https://www.doi.org/10.1073/pnas.1714348115
601 28. Li M, Hener P, Zhang Z, Kato S, Metzger D, Chambon P. Topical vitamin D3 and low-
602 calcemic analogs induce thymic stromal lymphopoietin in mouse keratinocytes and
603 trigger an atopic dermatitis. Proc Natl Acad Sci U S A [Internet]. 2006 Aug
604 1;103(31):11736–41. Available from:
605 http://www.ncbi.nlm.nih.gov/pubmed/16880407
606 29. Sullivan BM, Liang H-E, Bando JK, Wu D, Cheng LE, McKerrow JK, et al. Genetic
607 analysis of basophil function in vivo. Nat Immunol [Internet]. 2011 Jun 8 [cited 2013
608 Mar 23];12(6):527–35. Available from: https://www.doi.org/10.1038/ni.2036
609 30. Pellefigues C, Mehta P, Prout MS, Naidoo K, Yumnam B, Chandler J, et al. The
610 Basoph8 Mice Enable an Unbiased Detection and a Conditional Depletion of
611 Basophils. Front Immunol [Internet]. 2019 Sep 10 [cited 2019 Sep 11];10:2143.
612 Available from: https://www.doi.org/10.3389/fimmu.2019.02143
613 31. Abram CL, Roberge GL, Hu Y, Lowell CA. Comparative analysis of the efficiency and

specificity of myeloid-Cre deleting strains using ROSA-EYFP reporter mice. J Immunol Methods [Internet]. 2014 Jun [cited 2018 Nov 7];408:89–100. Available from: http://dx.doi.org/10.1016/j.jim.2014.05.009

32. Jacobsen EA, Lesuer WE, Willetts L, Zellner KR, Mazzolini K, Antonios N, et al. Eosinophil activities modulate the immune/inflammatory character of allergic respiratory responses in mice. Allergy [Internet]. 2014 Mar;69(3):315–27. Available from: http://www.ncbi.nlm.nih.gov/pubmed/24266710

33. Hu-Li J, Pannetier C, Guo L, Löhning M, Gu H, Watson C, et al. Regulation of Expression of IL-4 Alleles. Immunity [Internet]. 2001 Jan;14(1):1–11. Available from: https://linkinghub.elsevier.com/retrieve/pii/S107476130100084X

34. Roediger B, Kyle R, Yip KH, Sumaria N, Guy T V, Kim BS, et al. Cutaneous immunosurveillance and regulation of inflammation by group 2 innate lymphoid cells. Nat Immunol [Internet]. 2013 Jun 21;14(6):564–73. Available from: https://www.doi.org/10.1038/ni.2584

35. Harris SE, MacDougall M, Horn D, Woodruff K, Zimmer SN, Rebel VI, et al. Meox2Cre-mediated disruption of CSF-1 leads to osteopetrosis and osteocyte defects. Bone [Internet]. 2012 Jan [cited 2019 Jul 18];50(1):42–53. Available from: http://www.ncbi.nlm.nih.gov/pubmed/21958845

36. Al-Shami A, Spolski R, Kelly J, Fry T, Schwartzberg PL, Pandey A, et al. A Role for Thymic Stromal Lymphopoietin in CD4+ T Cell Development. J Exp Med [Internet]. 2004 Jul 19;200(2):159–68. Available from: https://rupress.org/jem/article/200/2/159/40115/A-Role-for-Thymic-Stromal-Lymphopoietin-in-CD4-T

37. Köntgen F, Süss G, Stewart C, Steinmetz M, Bluethmann H. Targeted disruption of the

MHC class II Aa gene in C57BL/6 mice. Int Immunol [Internet]. 1993;5(8):957–64. Available from: https://academic.oup.com/intimm/article-lookup/doi/10.1093/intimm/5.8.957

38. Naidoo K, Jagot F, van den Elsen L, Pellefigues C, Jones A, Luo H, et al. Eosinophils determine dermal thickening and water loss in a MC903 model of atopic dermatitis. J Invest Dermatol [Internet]. 2018; Available from: http://www.ncbi.nlm.nih.gov/pubmed/29964034%0A

39. Schmidt AJ, Mayer JU, Wallace PK, Ronchese F, Price KM. Simultaneous Polychromatic Immunofluorescent Staining of Tissue Sections and Consecutive Imaging of up to Seven Parameters by Standard Confocal Microscopy. Curr Protoc Cytom [Internet]. 2019 Dec 24;91(1). Available from: https://onlinelibrary.wiley.com/doi/abs/10.1002/cpcy.64

40. Pellefigues C, Dema B, Lamri Y, Saidoune F, Chavarot N, Lohéac C, et al. Prostaglandin D2 amplifies lupus disease through basophil accumulation in lymphoid organs. Nat Commun [Internet]. 2018 Dec 20;9(1):725. Available from: https://www.doi.org/10.1038/s41467-018-03129-8

41. Ferrer-Font L, Pellefigues C, Mayer JU, Small SJ, Jaimes MC, Price KM. Panel Design and Optimization for High-Dimensional Immunophenotyping Assays Using Spectral Flow Cytometry. Curr Protoc Cytom [Internet]. 2020;92(1):1–25. Available from: https://doi.org/10.1002/cpcy.70

42. Moll R, Divo M, Langbein L. The human keratins: biology and pathology. Histochem Cell Biol [Internet]. 2008 Jun;129(6):705–33. Available from: http://www.ncbi.nlm.nih.gov/pubmed/18461349

43. Madsen L, Labrecque N, Engberg J, Dierich A, Svejgaard A, Benoist C, et al. Mice

662 lacking all conventional MHC class II genes. Proc Natl Acad Sci U S A [Internet]. 1999
663 Aug 31;96(18):10338–43. Available from:
664 http://www.ncbi.nlm.nih.gov/pubmed/10468609
665 44. Samuelov L, Sarig O, Harmon RM, Rapaport D, Ishida-Yamamoto A, Isakov O, et al.
666 Desmoglein 1 deficiency results in severe dermatitis, multiple allergies and metabolic
667 wasting. Nat Genet [Internet]. 2013 Oct;45(10):1244–8. Available from:
668 http://www.ncbi.nlm.nih.gov/pubmed/23974871
669 45. Pellerin L, Henry J, Hsu CY, Balica S, Jean-Decoster C, Méchin MC, et al. Defects of
670 filaggrin-like proteins in both lesional and nonlesional atopic skin. J Allergy Clin
671 Immunol. 2013;131(4):1094–102.
672 46. Zeng MY, Pham D, Bagaitkar J, Liu J, Otero K, Shan M, et al. An efferocytosis-induced,
673 IL-4–dependent macrophage-iNKT cell circuit suppresses sterile inflammation and is
674 defective in murine CGD. Blood [Internet]. 2013 Apr 25 [cited 2018 Jul
675 27];121(17):3473–83. Available from:
676 http://www.ncbi.nlm.nih.gov/pubmed/23426944
677 47. Jenkins SJ, Ruckerl D, Thomas GD, Hewitson JP, Duncan S, Brombacher F, et al. IL-4
678 directly signals tissue-resident macrophages to proliferate beyond homeostatic levels
679 controlled by CSF-1. J Exp Med [Internet]. 2013 Oct 21;210(11):2477–91. Available
680 from: http://www.jem.org/lookup/doi/10.1084/jem.20121999
681 48. A-Gonzalez N, Quintana JA, García-Silva S, Mazariegos M, González de la Aleja A,
682 Nicolás-Ávila JA, et al. Phagocytosis imprints heterogeneity in tissue-resident
683 macrophages. J Exp Med [Internet]. 2017 May 1 [cited 2019 Apr 20];214(5):1281–96.
684 Available from: http://www.ncbi.nlm.nih.gov/pubmed/28432199
685 49. Serhan CN. Pro-resolving lipid mediators are leads for resolution physiology. Nature

[Internet]. 2014 Jun 5 [cited 2014 Dec 5];510(7503):92–101. Available from: http://www.ncbi.nlm.nih.gov/pubmed/24899309

50. Isobe Y, Kato T, Arita M. Emerging Roles of Eosinophils and Eosinophil-Derived Lipid Mediators in the Resolution of Inflammation. Front Immunol [Internet]. 2012;3. Available from: http://journal.frontiersin.org/article/10.3389/fimmu.2012.00270/abstract

51. Gundra UM, Girgis NM, Ruckerl D, Jenkins S, Ward LN, Kurtz ZD, et al. Alternatively activated macrophages derived from monocytes and tissue macrophages are phenotypically and functionally distinct. Blood [Internet]. 2014 May 15;123(20):e110-22. Available from: http://www.ncbi.nlm.nih.gov/pubmed/24695852

52. Heng TSP, Painter MW, Immunological Genome Project Consortium. The Immunological Genome Project: networks of gene expression in immune cells. Nat Immunol [Internet]. 2008 Oct;9(10):1091–4. Available from: http://www.ncbi.nlm.nih.gov/pubmed/18800157

53. McQuin C, Goodman A, Chernyshev V, Kamentsky L, Cimini BA, Karhohs KW, et al. CellProfiler 3.0: Next-generation image processing for biology. PLoS Biol [Internet]. 2018;16(7):e2005970. Available from: https://doi.org/10.1371/journal.pbio.2005970

54. Hamilton TA, Zhao C, Pavicic PG, Datta S. Myeloid Colony-Stimulating Factors as Regulators of Macrophage Polarization. Front Immunol [Internet]. 2014 Nov 21;5. Available from: http://journal.frontiersin.org/article/10.3389/fimmu.2014.00554/abstract

55. Saunders SP, Moran T, Floudas A, Wurlod F, Kaszlikowska A, Salimi M, et al. Spontaneous atopic dermatitis is mediated by innate immunity, with the secondary lung inflammation of the atopic march requiring adaptive immunity. J Allergy Clin

Immunol [Internet]. 2016 Feb;137(2):482–91. Available from: http://www.ncbi.nlm.nih.gov/pubmed/26299987

56. Hendricks AJ, Eichenfield LF, Shi VY. The impact of airborne pollution on atopic dermatitis: a literature review. Br J Dermatol [Internet]. 2020 Jul 15;183(1):16–23. Available from: https://onlinelibrary.wiley.com/doi/abs/10.1111/bjd.18781

57. Brunner PM, Israel A, Zhang N, Leonard A, Wen H-C, Huynh T, et al. Early-onset pediatric atopic dermatitis is characterized by T H 2/T H 17/T H 22-centered inflammation and lipid alterations. J Allergy Clin Immunol [Internet]. 2018 Jun [cited 2018 Aug 7];141(6):2094–106. Available from: https://linkinghub.elsevier.com/retrieve/pii/S0091674918303932

58. Flohr C, Johansson SG., Wahlgren C-F, Williams H. How atopic is atopic dermatitis? J Allergy Clin Immunol [Internet]. 2004 Jul;114(1):150–8. Available from: https://linkinghub.elsevier.com/retrieve/pii/S0091674904013946

59. Illi S, von Mutius E, Lau S, Nickel R, Grüber C, Niggemann B, et al. The natural course of atopic dermatitis from birth to age 7 years and the association with asthma☆ J Allergy Clin Immunol [Internet]. 2004 May;113(5):925–31. Available from: https://linkinghub.elsevier.com/retrieve/pii/S0091674904009947

60. Pellefigues C. IgE Autoreactivity in Atopic Dermatitis: Paving the Road for Autoimmune Diseases? Antibodies [Internet]. 2020 Sep 8;9(3):47. Available from: https://www.mdpi.com/2073-4468/9/3/47

61. Leyva-Castillo JM, Hener P, Jiang H, Li M. TSLP Produced by Keratinocytes Promotes Allergen Sensitization through Skin and Thereby Triggers Atopic March in Mice. J Invest Dermatol [Internet]. 2013;133(1):154–63. Available from: http://www.sciencedirect.com/science/article/pii/S0022202X15359662

734 62. Simpson EL, Parnes JR, She D, Crouch S, Rees W, Mo M, et al. Tezepelumab, an anti–
735 thymic stromal lymphopoietin monoclonal antibody, in the treatment of moderate to
736 severe atopic dermatitis: A randomized phase 2a clinical trial. J Am Acad Dermatol
737 [Internet]. 2019 Apr;80(4):1013–21. Available from:
738 https://linkinghub.elsevier.com/retrieve/pii/S0190962218330500
739 63. Voehringer D. Basophil modulation by cytokine instruction. Eur J Immunol [Internet].
740 2012;42(10):2544–50. Available from: https://doi.org/10.1002/eji.201142318
741 64. Ricardo-Gonzalez RR, Van Dyken SJ, Schneider C, Lee J, Nussbaum JC, Liang HE, et al.
742 Tissue signals imprint ILC2 identity with anticipatory function. Nat Immunol. 2018 Oct
743 1;19(10):1093–9.
744 65. Junttila IS, Watson C, Kummola L, Chen X, Hu-Li J, Guo L, et al. Efficient cytokine-
745 induced IL-13 production by mast cells requires both IL-33 and IL-3. J Allergy Clin
746 Immunol [Internet]. 2013 Sep;132(3):704-712.e10. Available from:
747 https://www.doi.org/10.1016/j.jaci.2013.03.033
748 66. Noti M, Wojno EDT, Kim BS, Siracusa MC, Giacomin PR, Nair MG, et al. Thymic
749 stromal lymphopoietin-elicited basophil responses promote eosinophilic esophagitis.
750 Nat Med [Internet]. 2013 Aug [cited 2014 Oct 16];19(8):1005–13. Available from:
751 http://www.ncbi.nlm.nih.gov/pubmed/23872715
752 67. Cohen M, Giladi A, Gorki A-DD, Solodkin DG, Zada M, Hladik A, et al. Lung Single-Cell
753 Signaling Interaction Map Reveals Basophil Role in Macrophage Imprinting. Cell
754 [Internet]. 2018 Nov 1 [cited 2018 Dec 4];175(4):1031-1044.e18. Available from:
755 https://doi.org/10.1016/j.cell.2018.09.009
756 68. Nakashima C, Otsuka A, Kitoh A, Honda T, Egawa G, Nakajima S, et al. Basophils
757 regulate the recruitment of eosinophils in a murine model of irritant contact

dermatitis. J Allergy Clin Immunol [Internet]. 2014;134(1):100-107.e12. Available from: http://dx.doi.org/10.1016/j.jaci.2014.02.026

69. Schiechl G, Hermann FJ, Rodriguez Gomez M, Kutzi S, Schmidbauer K, Talke Y, et al. Basophils Trigger Fibroblast Activation in Cardiac Allograft Fibrosis Development. Am J Transplant [Internet]. 2016 Sep 1 [cited 2020 Feb 10];16(9):2574–88. Available from: http://doi.wiley.com/10.1111/ajt.13764

70. Cheng LE, Sullivan BM, Retana LE, Allen CDC, Liang H-E, Locksley RM. IgE-activated basophils regulate eosinophil tissue entry by modulating endothelial function. J Exp Med [Internet]. 2015;212(4):513–24. Available from: http://jem.rupress.org/content/212/4/513.abstract

71. Salimi M, Barlow JL, Saunders SP, Xue L, Gutowska-Owsiak D, Wang X, et al. A role for IL-25 and IL-33-driven type-2 innate lymphoid cells in atopic dermatitis. J Exp Med [Internet]. 2013;210(13):2939–50. Available from: http://www.pubmedcentral.nih.gov/articlerender.fcgi?artid=3865470&tool=pmcentrez&rendertype=abstract

Figure titles and Legends

Fig. 1: MC903 induces an AD-like resolving epidermal disease. C57BL/6 mice ears were treated with 4nmol MC903 or EtOH daily for 4 days. (A) Ear thickness and transepidermal water loss (TEWL) were monitored over time (n=27). (B) Representative pictures of the ear skin. (C) Representative H&E staining (scale = 50µm, 20X) and (D) quantification of dermal and epidermal thickness (n=5, 5 Fields of view (FOV)/ear). (E) Representative Masson's

782 trichrome stained ear tissue sections at day 9 and day 12 (scale = 50µm, 20X) and (F)
783 quantification of the dermal area of collagen (n= 8, 6-8 FOV/ear 20X). (G) Representative 3D
784 reconstruction of Ki67, keratin 14 and 10 (K14, K10) and filaggrin (FLG) immunofluorescent
785 staining of the ear skin (40X) and quantification of the area of (H) K14, (I) K10, (J) K14+ Ki67+
786 keratinocytes, (K) the area of filaggrin and the (L) number of FLG+ cells (H-K: n=4, L: n=3; 5
787 FOV/ear). Results are from 5 (A, B), 2 (F-K) or (D, L) are representative of at least 2
788 independent experiments. Means +/- SEM are represented. (D, F, H-L) Statistics are one-way
789 ANOVA with Tukey's post-test. *: $p<0.05$; **: $p<0.01$; ***: $p<0.001$; ****: $p<0.0001$
790
791 **Fig. 2: Basophils are the main source of type 2 cytokines in AD skin**. B8x4C13R female mice
792 were treated with MC903 and skin leucocytes analysed by flow cytometry. (A) Contour and
793 pseudocolor plots of a representative t-SNE analysis of the kinetics of skin leucocytes
794 populations (10k $CD45^+$/mouse, 4 mice/day). Clusters were numbered and immune cells
795 identified in each cluster. (B) Kinetics of selected leucocytes are depicted (n=10). (C) Overall
796 expression of IL-4 (AmCyan) and IL-13 (dsRed) from D0 to D12 (as in A) in heatmap of
797 intensity of expression. (D) Representative dot plots showing the expression of IL-4 and IL-
798 13 by basophils, ILC2s or $CD4^+$ T cells at Day 9. (E) Quantification of the number of IL-4 or IL-
799 13+ cells (n=10) or (F) Il4 and Il13 transcripts in the ear (n= 4, 5, 5, 10) overtime. Results are
800 representative of at least two independent experiments showing similar results. (B) Means
801 +/- SEM or (E, F) medians and interquartile ranges are represented. (F) Statistics are a two
802 way ANOVA with Sidak's multiple comparison. *: $p<0.05$; ****: $p<0.0001$
803

804 **Fig. 3: Basophil derived IL-4 controls epidermal barrier function and differentiation.**

805 B8xiDTR or IL-4^{KO} mice were treated with MC903 or EtOH, and diphtheria toxin (DT) or PBS.

806 (A) Ear swelling and TEWL monitoring (n = 8, 12 , 12, 14). (B) Gene expression of *Il4* (n=14,

807 17) and (C) *Il13* in the earat D9 (n=10, 10, 12) ND: Not detected. (D) Dermal and epidermal

808 thickness assessed on H&E sections (n=3, 4, 4, 4, 6-7 Fields of view (FOV) / ear) at D0 or D9.

809 (E) Number of keratin 10+ (K10),Filaggrin+ (Flg+) cells assessed at 40X (n=4, 5-6 FOV/ear). (F)

810 K14+ Ki67+ cells (n=5, 5-6 FOV/ear) and keratin 14 area (n=4, 5-6 FOV/ear) at 20X at D9. (G)

811 C57BL/6 ear gene expression overtime (n=6-10) and at D9 (n=10-20). (A, E, F) Means +/-

812 SEM or (B, C, G) medians and violin plots are represented. (A, F) Representative of, or (B - E,

813 G) from at least two independent experiments. Statistics are (A) two-way ANOVA with a

814 Sidak's or (D) a Kruskall-Wallis or (E, F) one-way ANOVAs with a Dunnett's post-test and (B,

815 C, G) Mann Whitney tests. ns: non- significant. *: $p<0.05$; **: $p<0.01$; ***: $p<0.001$; ****:

816 $p<0.0001$

817 **Fig. 4: Basophil derived IL-4 promotes a pro-resolution leucocyte landscape during**

818 **inflammation**. B8.4C13RxiDTR mice were treated with MC903 with or without diphtheria

819 toxin (DT) until D9. Ear CD45+ cells were analysed by flow cytometry. (A) Representative t-

820 SNE analysis of skin leucocytes populations at D9 (20k CD45+ / mouse, n=5), showing

821 leucocyte clusters, (B)and overlay of DT treated (Red) and untreated mice (Black), revealing

822 depleted clusters. The proportion of (C) granulocytes and relevant lymphoid cells (n=13-17),

823 (D) Ly6C+ monocytes or macrophages (n=13-22), (E) CD206^{hi} or MHCII^{hi} macrophages (n=6 -

824 12) and (F) the expression of IL-4 (AmCyan) by CD206^{hi} macrophages (n=19-23), (G) CD4+ T

825 cells, or expression of IL-13 (dsRed) by CD4+ T cells and ILC2s (n=10-13) was analysed at Day

826 9 after EtOH (-) or MC903 treatment without (PBS) or with DT (DT) in B8.4C13RxiDTR or IL-

4KO ($IL4^{ko}$) mice. (H) Gene expression of Relm-α and Arginase 1 was analysed overtime (n=6-17) and at D9 (n=10-12) by qPCR in the whole ear skin. Medians are represented. (A, B) Representative of two or (C to H) from three independent experiments showing similar results. Statistics are Kruskall Wallis with a Dunn's post-test. #: p<0.1; *: p<0.05; **: p<0.01; ***: p<0.001; ****: p<0.0001

Fig. 5: Basophils control dermal resident macrophage efferocytosis. B8xiDTR mice were treated with EtOH (-) or MC903 for 4 days. MC903 treated mice were depleted of basophils by injections of diphteria toxin (DT) or not (PBS). At D9 after MC903 treatment, 2M dsRed+ apoptotic cells were injected in the ear dermis. 2hr later mice were sacrificed and ear cells analysed by flow cytometry. (A) Representative gating strategy of skin phagocytes and their uptake of dsRed+ apoptotic cells. (B) Histograms representing the efferocytosis of macrophages and relevant subsets as in (A), (n=6-8). (C) EtOH or MC903 treated ears were analysed by immunofluorescence for macrophages and apoptotic cell content by TUNEL assay (AF: autofluorescence, scale =50µm), and the TUNEL+ area was quantified (n=5-7 mice with 10 Field of view (FOV) per mouse). Results are (A, B) representative of or (C) pooled from two independent experiments showing similar results. Means +/- SEM are represented. Statistics are unpaired t-tests. ns: non-significant. *: p<0.05; **: p<0.01; ****: p<0.0001

Fig. 6: Basophils show anti-inflammatory and pro-remodeling properties during the resolution phase. B8.iDTRx4C13R mice were treated with MC903 or EtOH on the contralateral ear and injected with diphtheria toxin (DT) or PBS (PBS) daily from D8. At D12 (A-C) ear skin leucocytes wereanalyzed by flow cytometry (n=5-9). (D) Whole skin

transcripts of relevant genes were analyzed by qPCR (n=8-16). (E) Dermal and epidermal hyperplasia was quantified on H&E sections (n=8 ears with 5-7 sections /ear), (F) filaggrin (FLG+), keratin 14 (K14+) and keratin 10 (K10+) cells counted from immunofluorescence sections (n=3 mice, 8 Fields of view (FOV) / ear) and (G) collagen content was determined on Masson's trichrome sections (n= 8 ears with 6-7 section /ear). Results are (B, C, F) representative or (A, E, G) pooled from two to three independent experiments showing similar results. (A-C) Medians and interquartile range or (D, G) in violin plots, or (E, F) means +/- SEM are represented. Statistics are (A-D, G) Mann-Whitney or (E, F) unpaired t-tests. Ns: non-significant. #: p<0.1; *: p<0.05; **: p<0.01; ***: p<0.001; ****: p<0.0001

Fig. 7: Basophil derived IL-4 and M-CSF support the resolution of inflammation. C57BL/6J were treated with MC903 or EtOH on both ears and injected intraperitoneally with anti-IL-4 (a-IL4) or rat IgG1 (iso) or PBS at D9 and D11 and (A) their ear swelling and TEWL were monitored overtime (n= 22, 26, 26, 26), and (B) skin leucocytes analysed at D12 by FACS (n=17,19,19). $B8^{tg/wt}.CSF1^{fl/fl}$ ($CSF1^{\Delta MCPT8}$) and $B8^{wt/wt}.CSF1^{fl/fl}$ ($CSF1^{fl/fl}$) littermates were treated with MC903 and EtOH on the contralateral ear and (C) the ear swelling and TEWL of males (n= 13 and 16) and (D) females (n= 20 and 19 for MC903, 15 and 9 for EtOH) was monitored. (e) Skin leucocytes populations were quantified by FACS in female mice at D12 (n=12, 12, 17, 17). (A, C, D) Means +/- SEM or (B, E) medians and interquartile range are represented. Statistics are (A, C, D) two-way ANOVAs with a Tukey's post-test comparing each MC903 treated genotype and (B, E) Mann-Whitney tests. Results are from (A, B, E) two or (C, D) three independent experiments. ns: non-significant. *: p<0.05; **: p<0.01; ***: p<0.001; ****: p<0.0001

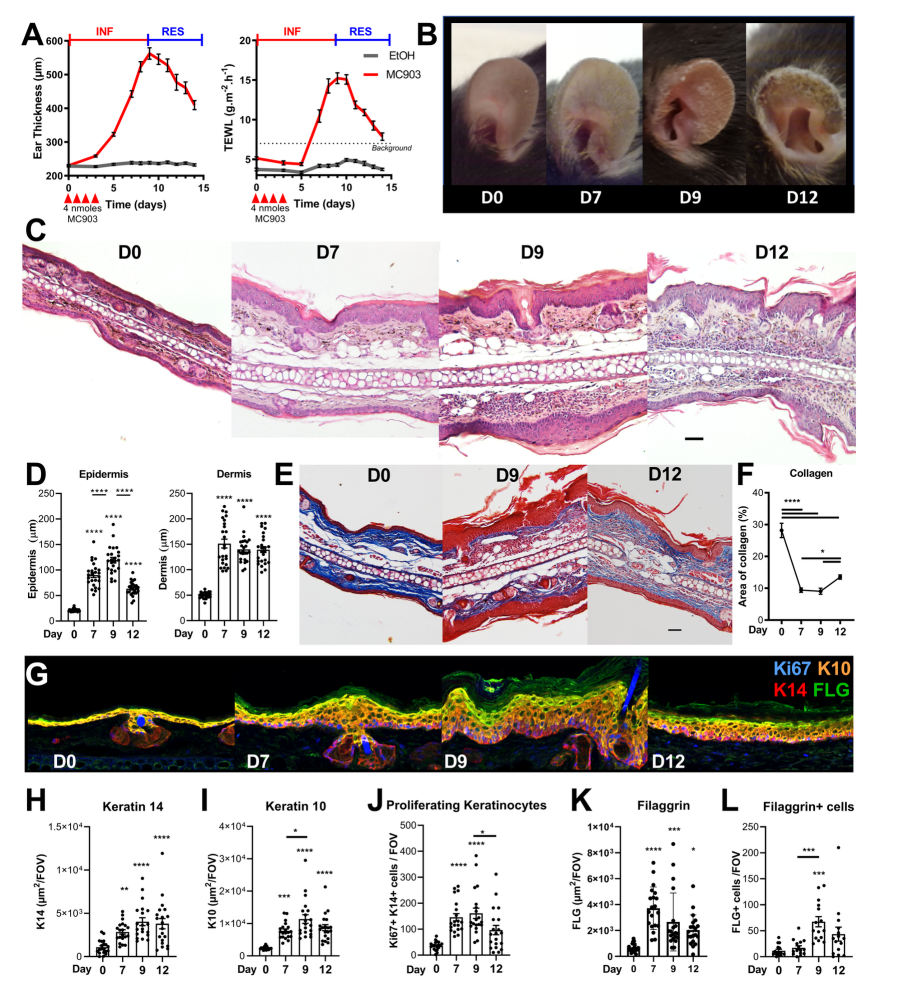
A
INF
RES
Ear Thickness (µm)
Time (days)
4 nmoles MC903
EtOH
MC903
TEWL (g.m-2.h-1)
Background
B
D0
D7
D9
D12
C
D0
D7
D9
D12
D
Epidermis
Dermis
Epidermis (µm)
Dermis (µm)
Day
E
D0
D9
D12
F
Collagen
Area of collagen (%)
Day
G
Ki67 K10
K14 FLG
D0
D7
D9
D12
H
Keratin 14
K14 (µm2/FOV)
I
Keratin 10
K10 (µm2/FOV)
J
Proliferating Keratinocytes
Ki67+ K14+ cells / FOV
K
Filaggrin
FLG (µm2/FOV)
L
Filaggrin+ cells
FLG+ cells /FOV

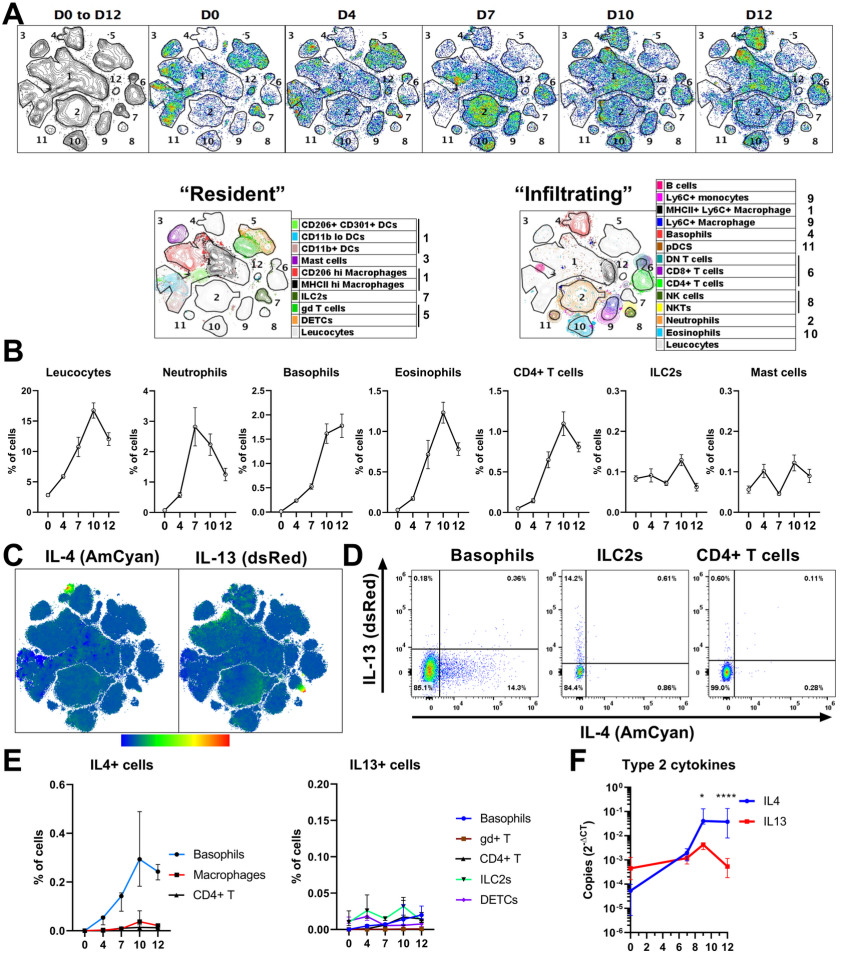
A
D0 to D12
D0
D4
D7
D10
D12
"Resident"
CD206+ CD301+ DCs
CD11b lo DCs
CD11b+ DCs
Mast cells
CD206 hi Macrophages
MHCII hi Macrophages
ILC2s
gd T cells
DETCs
Leucocytes
1
3
1
7
5
"Infiltrating"
B cells
Ly6C+ monocytes
MHCII+ Ly6C+ Macrophage
Ly6C+ Macrophage
Basophils
pDCS
DN T cells
CD8+ T cells
CD4+ T cells
NK cells
NKTs
Neutrophils
Eosinophils
Leucocytes
9
1
9
4
11
6
8
2
10
B
Leucocytes
Neutrophils
Basophils
Eosinophils
CD4+ T cells
ILC2s
Mast cells
% of cells
C
IL-4 (AmCyan)
IL-13 (dsRed)
D
Basophils
ILC2s
CD4+ T cells
IL-13 (dsRed)
IL-4 (AmCyan)
0.18%
0.36%
85.1%
14.3%
14.2%
0.61%
84.4%
0.86%
0.60%
0.11%
99.0%
0.28%
E
IL4+ cells
IL13+ cells
% of cells
Basophils
Macrophages
CD4+ T
gd+ T
ILC2s
DETCs
F
Type 2 cytokines
Copies (2^-ΔCT)
IL4
IL13
*
****

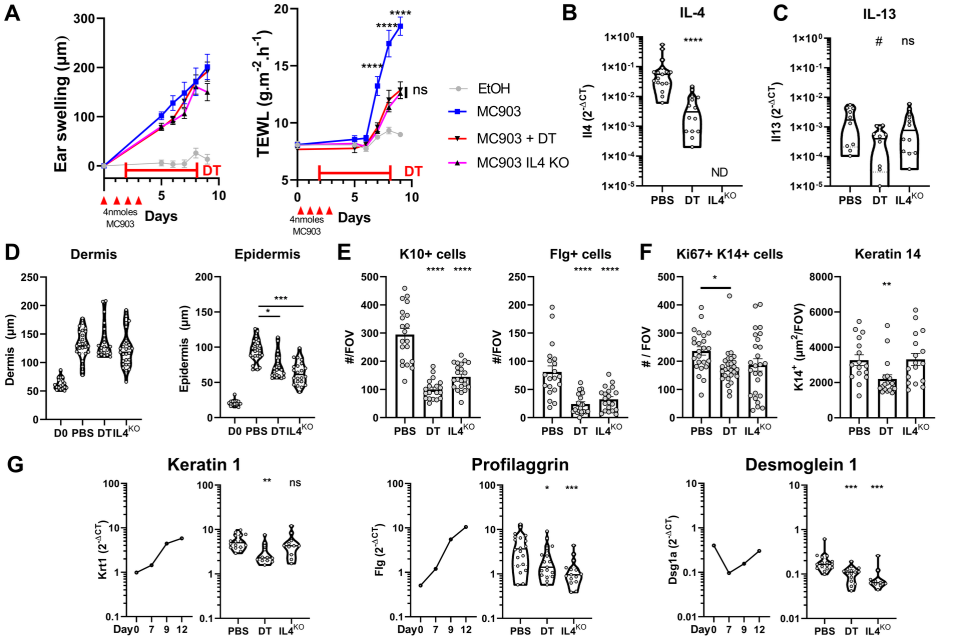
A
Ear swelling (µm)
Days
4nmoles MC903
TEWL (g.m-2.h-1)
ns
DT
EtOH
MC903
MC903 + DT
MC903 IL4 KO
B
IL-4
Il4 (2-ΔCT)
ND
PBS DT IL4KO
C
IL-13
Il13 (2-ΔCT)
#
ns
D
Dermis
Dermis (µm)
Epidermis
Epidermis (µm)
D0 PBS DT IL4KO
E
K10+ cells
#/FOV
Flg+ cells
F
Ki67+ K14+ cells
/ FOV
Keratin 14
K14+ (µm2/FOV)
G
Keratin 1
Krt1 (2-ΔCT)
Day0 7 9 12
Profilaggrin
Flg (2-ΔCT)
Desmoglein 1
Dsg1a (2-ΔCT)

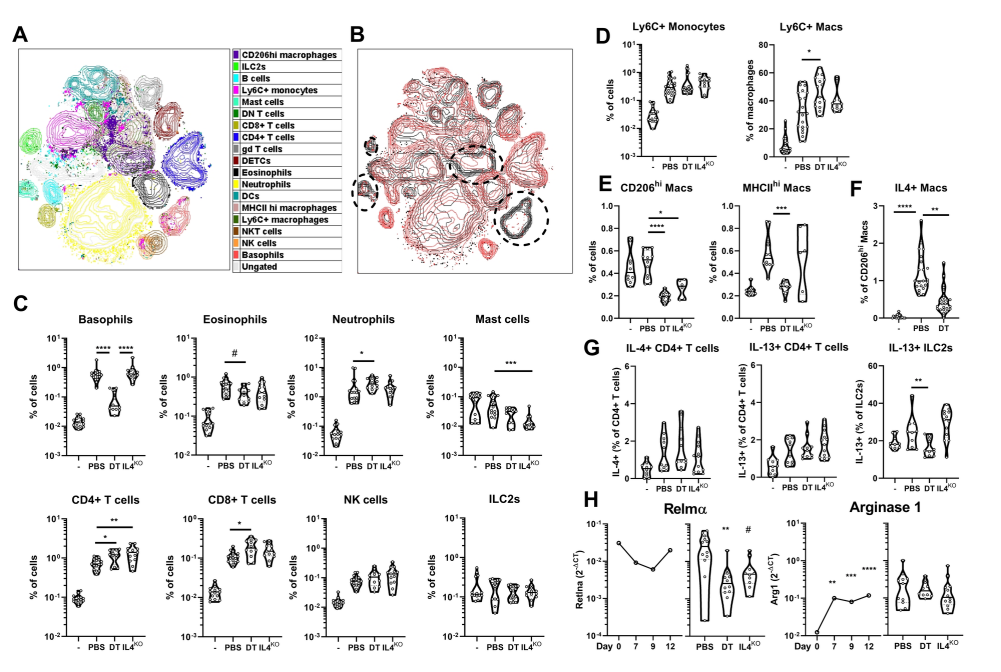
A
CD206hi macrophages
ILC2s
B cells
Ly6C+ monocytes
Mast cells
DN T cells
CD8+ T cells
CD4+ T cells
gd T cells
DETCs
Eosinophils
Neutrophils
DCs
MHCII hi macrophages
Ly6C+ macrophages
NKT cells
NK cells
Basophils
Ungated
B
C
Basophils
Eosinophils
Neutrophils
Mast cells
CD4+ T cells
CD8+ T cells
NK cells
ILC2s
% of cells
- PBS DT IL4KO
D
Ly6C+ Monocytes
Ly6C+ Macs
% of cells
% of macrophages
- PBS DT IL4KO
E
CD206hi Macs
MHCIIhi Macs
% of cells
- PBS DT IL4KO
F
IL4+ Macs
% of CD206hi Macs
- PBS DT
G
IL-4+ CD4+ T cells
IL-13+ CD4+ T cells
IL-13+ ILC2s
IL-4+ (% of CD4+ T cells)
IL-13+ (% of CD4+ T cells)
IL-13+ (% of ILC2s)
- PBS DT IL4KO
H
Relmα
Arginase 1
Retnla (2-ΔCT)
Arg1 (2-ΔCT)
Day 0 7 9 12
PBS DT IL4KO

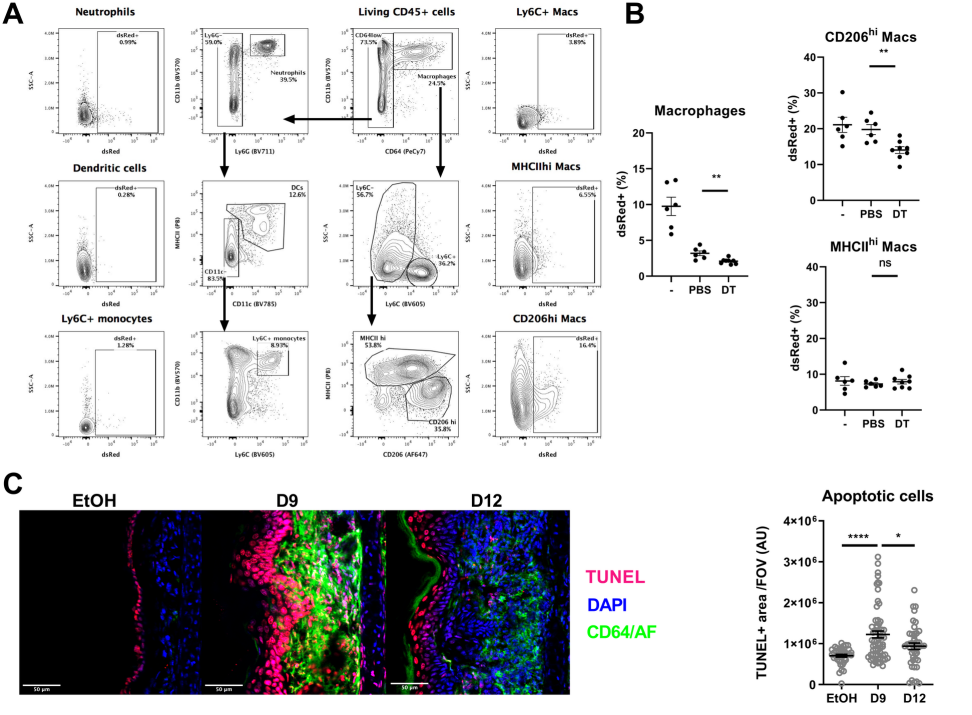
A
Neutrophils
dsRed+
0.99%
Ly6G-
59.0%
Neutrophils
39.5%
Ly6G (BV711)
CD11b (BV570)
SSC-A
dsRed
Living CD45+ cells
CD64 Hi
73.5%
Macrophages
24.5%
CD64 (PeCy7)
Ly6C+ Macs
dsRed+
3.89%
Dendritic cells
dsRed+
0.28%
DCs
12.6%
CD11c
83.5%
CD11c (BV785)
MHCII (PE)
MHCIIhi Macs
Ly6C-
56.7%
Ly6C+
36.2%
Ly6C (BV605)
dsRed+
6.55%
Ly6C+ monocytes
dsRed+
1.28%
Ly6C+ monocytes
8.93%
Ly6C (BV605)
CD206hi Macs
MHCII hi
53.8%
CD206 hi
35.8%
CD206 (AF647)
dsRed+
16.4%
B
Macrophages
dsRed+ (%)
**
-
PBS
DT
CD206hi Macs
**
MHCIIhi Macs
ns
C
EtOH
D9
D12
50 µm
TUNEL
DAPI
CD64/AF
Apoptotic cells
TUNEL+ area /FOV (AU)
4×10^6
3×10^6
2×10^6
1×10^6
0
****
*
EtOH
D9
D12

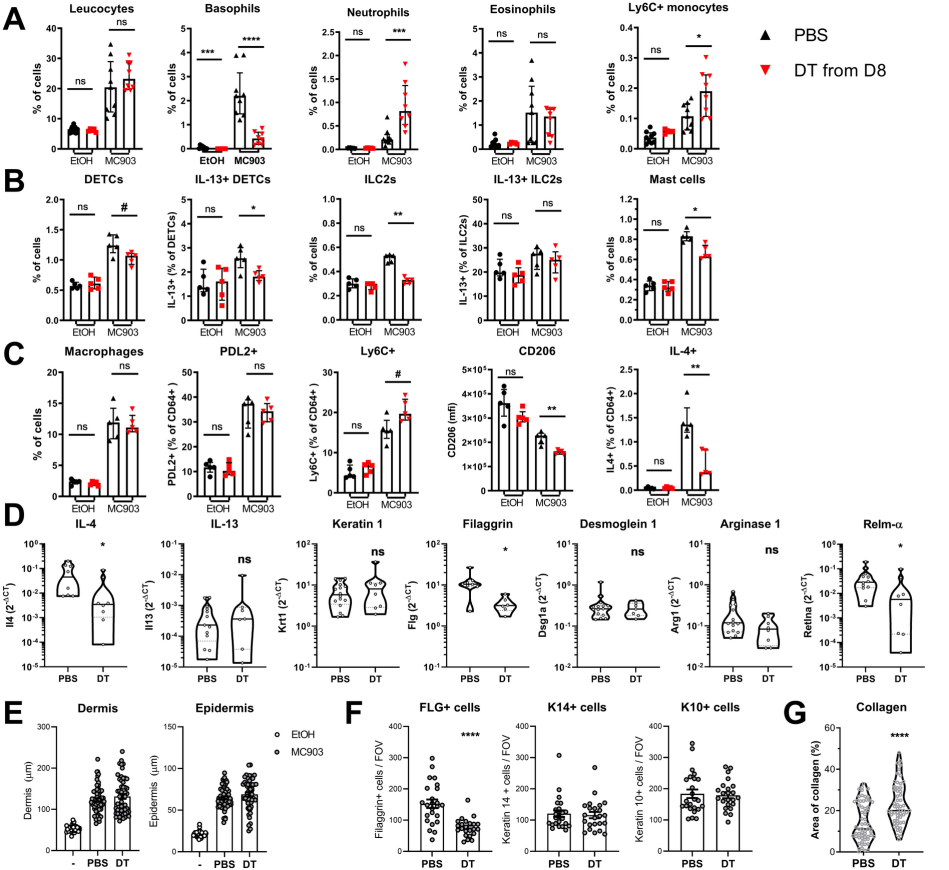
A
Leucocytes
Basophils
Neutrophils
Eosinophils
Ly6C+ monocytes
% of cells
EtOH
MC903
PBS
DT from D8
B
DETCs
IL-13+ DETCs
ILC2s
IL-13+ ILC2s
Mast cells
IL-13+ (% of DETCs)
IL-13+ (% of ILC2s)
C
Macrophages
PDL2+
Ly6C+
CD206
IL-4+
PDL2+ (% of CD64+)
Ly6C+ (% of CD64+)
CD206 (mfi)
IL4+ (% of CD64+)
D
IL-4
IL-13
Keratin 1
Filaggrin
Desmoglein 1
Arginase 1
Relm-α
Il4 (2-ΔCT)
Il13 (2-ΔCT)
Krt1 (2-ΔCT)
Flg (2-ΔCT)
Dsg1a (2-ΔCT)
Arg1 (2-ΔCT)
Retina (2-ΔCT)
PBS
DT
E
Dermis
Epidermis
Dermis (µm)
Epidermis (µm)
EtOH
MC903
F
FLG+ cells
K14+ cells
K10+ cells
Filaggrin+ cells / FOV
Keratin 14 + cells / FOV
Keratin 10+ cells / FOV
G
Collagen
Area of collagen (%)

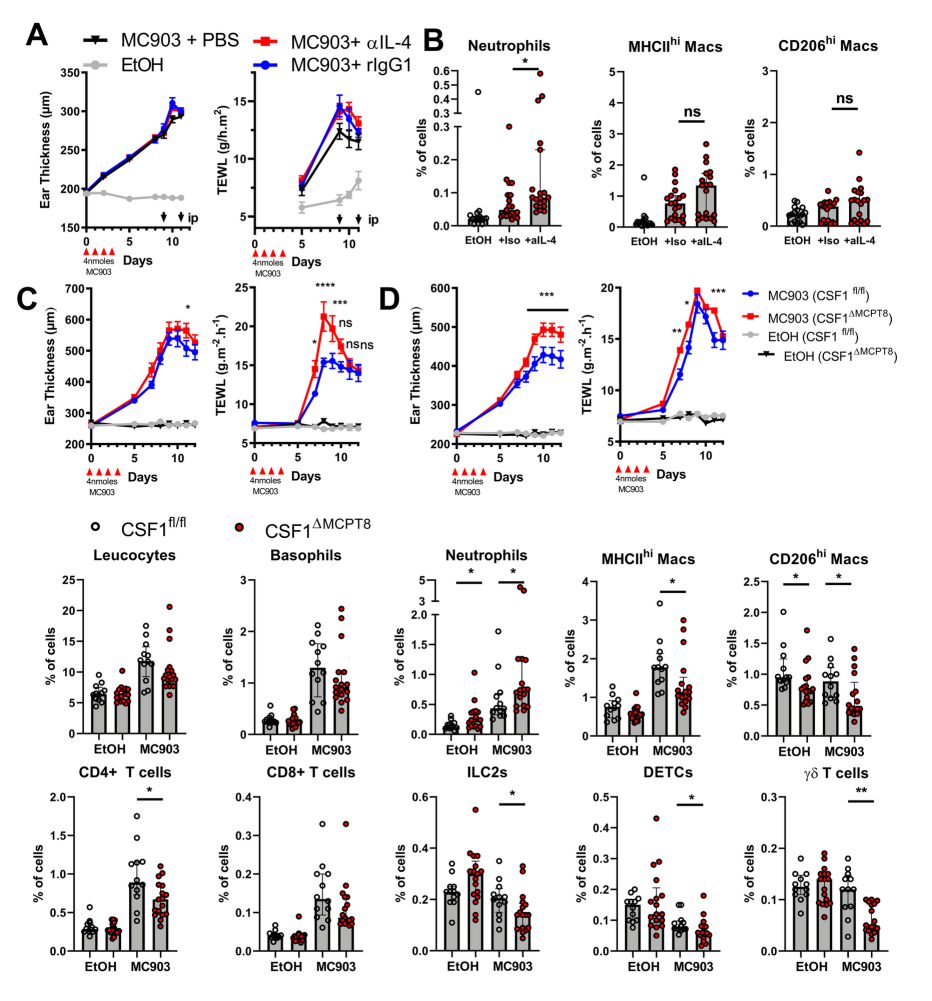
A
MC903 + PBS
EtOH
MC903+ αIL-4
MC903+ rIgG1
Ear Thickness (µm)
TEWL (g/h.m²)
ip
4nmoles MC903
Days
B
Neutrophils
MHCIIhi Macs
CD206hi Macs
% of cells
ns
EtOH
+Iso
+aIL-4
C
Ear Thickness (µm)
TEWL (g.m-2.h-1)
ns
Days
D
MC903 (CSF1 fl/fl)
MC903 (CSF1 ΔMCPT8)
EtOH (CSF1 fl/fl)
EtOH (CSF1 ΔMCPT8)
CSF1fl/fl
CSF1ΔMCPT8
Leucocytes
Basophils
Neutrophils
MHCIIhi Macs
CD206hi Macs
CD4+ T cells
CD8+ T cells
ILC2s
DETCs
γδ T cells
% of cells
EtOH
MC903

Basophil induces keratinocyte dysfunction and pro-resolution macrophages during atopic skin inflammation

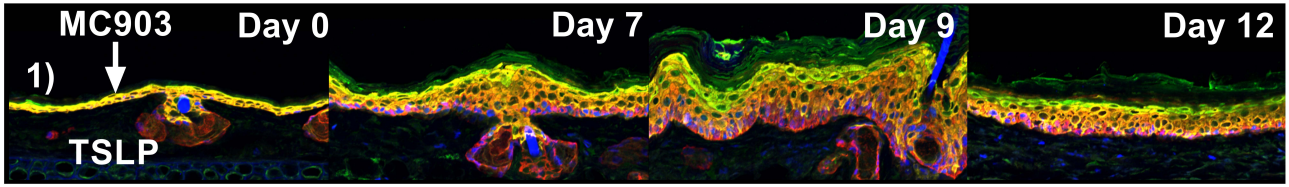

Bone marrow

Skin

4) Barrier dysfunction

5) Repair

Keratinocyte proliferation

Keratinocyte differentiation

+filaggrin, desmoglein

2)

3)

IL-4

IL-4
M-CSF

M2

Bφ IL-4

Bφ

4) Efferocytosis, Remodeling

Bφ: Basophils
M2: M2-like Macrophages

Direct evidence
Association

Pro-Inflammation
Pro-Resolution